should be possible, making these deflectors considerably faster than usual acoustooptic deflectors which have maximum speeds of 20-30 megapixels/s [8]. A typical acoustooptic deflector scans some hundred pixels with a total deflection of the order of 10 mrad. Hence, some of the dispersive deflectors shown in Table I have better performance than the ordinary acousto-optic deflector.

Conclusion

It has been shown that it is possible to construct fast beam deflectors based on usual dispersive optical components by means of electrooptic tuning of broad-band lasers. Scans with several thousand pixels, about 10 degrees of deflection and with scanning rates up to 10 gigapixels/s can be obtained.

References

[1] J. M. Telle and C. L. Tang, "New method for electrooptical tuning of tunable lasers," *Appl. Phys. Lett.*, vol. 24, pp. 85-87, 1974.
[2] "Electro-scan tuner," Ithaca Research Corp., Ithaca, NY.
[3] M. Born and E. Wolf, *Principles of Optics*, fifth edition. Oxford, England: Pergamon, 1975, p. 180.
[4] —, *Principles of Optics*, fifth edition. Oxford, England: Pergamon, 1975, p. 407.
[5] —, *Principles of Optics*, fifth edition. Oxford, England: Pergamon, 1975, pp. 403-406.
[6] —, *Principles of Optics*, fifth edition. Oxford, England: Pergamon, 1975, pp. 330-335.
[7] W. F. Hagen and P. C. Magnante, "Efficient second-harmonic generation with diffraction-limited and high-spectral radiance Nd-glass lasers," *J. Appl. Phys.*, vol. 40, pp. 219-224, 1969.
[8] B. R. Reddersen, "Highspeed acousto-optic scanning," *Laser Focus*, vol. 16, pp. 54-61, Oct. 1980.

Parametric Amplification and Frequency Conversion in Optical Fibers

ROGER H. STOLEN AND JOHN E. BJORKHOLM, SENIOR MEMBER, IEEE

(Invited Paper)

Abstract—**We find that the parametric four-photon gain for light pulses decreases for fibers longer than a characteristic length. This length is related to the common experimental observation that stimulated parametric emission is usually prominent only in short fibers while in long fibers stimulated Raman scattering dominates. Despite the fact that the actual process involves an intensity dependent bandwidth and broadening of the pump linewidth from self-phase modulation, it is possible to develop a simple expression for the characteristic length which requires only the initial pump linewidth and the low-power parametric bandwidth. This bandwidth can often be estimated from the pump wavelength and the measured frequency shift between the pump and the generated waves. Expressions for gain and amplification are derived from coupled wave equations and in the Appendixes it is shown that these are of the same form as the planewave equations, but modified by coupling coefficients called overlap integrals.**

I. Introduction

A WIDE variety of nonlinear optical effects have been observed using optical fibers as the nonlinear medium. Stimulated Raman scattering and four-photon parametric mixing can be used to convert the input light into light at one or more different frequencies [1]. In multimode fibers, both effects usually occur simultaneously although this need not necessarily be the case. In comparison with Raman frequency conversion, parametric frequency conversion is advantageous in that frequency up-conversion is possible as well as down-conversion, and the range of frequency shifts is broader. The same advantages apply when both processes are viewed as a means for amplifying light. A primary aim of this paper is to describe the circumstances which favor parametric output as opposed to Raman output. In particular, we treat the case of pulsed input light although much of the formalism is also applicable to the CW case.

The gain coefficient for four-photon parametric amplification is generally larger than that for stimulated Raman amplification. Consequently, the parametric output might be expected to always dominate over the Raman output. Using pulsed lasers, it has been observed experimentally that this is only true for fibers shorter than some characteristic length which we denote l_c. For fibers longer than l_c the stimulated Raman output dominates. In this paper we show how l_c can be evaluated and understood in terms of the frequency bandwidth of the parametric gain and self-phase modulation of the pulsed input light. We will only treat situations in which the shift between the frequencies of the generated light and the

Manuscript received January 7, 1982.
The authors are with Bell Laboratories, Holmdel, NJ 07733.

0018-9197/82/0700-1062$00.75

pump lies outside the Raman band so that parametric and Raman processes may be treated independently. When the frequency shift lies within the Raman band the parametric gain is slightly modified, but this additional contribution from the Raman susceptibility can be neglected in evaluating l_c.

Both parametric and Raman processes take advantage of the confinement of the optical fields and the long interaction lengths provided by low-loss fibers to reduce the pump power required for optical amplification [1]. Parametric amplification in a glass fiber absorbs two pump photons and, through the $\chi_3 E^3$ term in the polarization expansion, creates one photon higher in frequency than the pump and one lower in frequency than the pump. We refer to the low frequency wave as the Stokes wave and the higher frequency wave as the anti-Stokes wave. The third-order susceptibility χ_3 is complex with the real part leading to parametric gain and the imaginary part giving Raman Stokes gain and Raman anti-Stokes absorption. The second-order susceptibility χ_2 is zero in glass because of inversion symmetry.

The most important difference between the two processes is that the parametric process requires phasematching while Raman gain can be viewed as self-phasematched. There are several methods for achieving phasematching of the parametric interaction [2]-[13]. The most general approach is to use the different phase velocities of the waveguide modes in a multimode fiber [2]. One variation of this approach utilizes the birefringence in a polarization-preserving fiber [3]. Near the minimum dispersion wavelength around 1.3 μm, phasematching occurs in single-mode fibers due to the inflection in the index curve [4]. It is also possible to work with small frequency shifts ($\sim$1 cm^{-1}) where typical fiber lengths are shorter than the coherence length [5].

We first discuss some of the better understood phasematching techniques and their particular characteristics. Expressions for gain and amplification are then derived from coupled wave equations. These equations involve overlap integrals which are derived in Appendix A and discussed in Appendix B. There it is shown that nonlinear interactions between light waves propagating in the various modes of an optical fiber may be treated as interactions between uniform planewaves if the correct coupling coefficients are used.

The parametric gain bandwidth depends on pump intensity. There is also an intensity dependent shift of the maximum of the gain curve which is directly related to an intensity dependent refractive index. The inclusion of frequency broadening by self-phase modulation actually simplifies the problem leading to a straightforward method for choosing a fiber length l_c which will favor parametric scattering over stimulated Raman scattering. We will show that l_c depends only on the input pump linewidth and the parametric bandwidth which would be measured by low power mixing in a perfect fiber.

II. Phasematching Techniques for Four-Photon Mixing

Parametric interactions are strongest when the process is phasematched. Because of dispersion of the refractive indexes, however, phasematching is not generally obtained and the wavelength of the polarization produced by the mixing is slightly different from that of the corresponding free-running wave. Because of the resulting phase-slippage, after some distance called the coherence length l_{coh}, the free-running wave and the forced polarization will be 180° out of phase and energy will flow back into the pump wave. In general we have

$$l_{\text{coh}}(\Omega) = 2\pi/\Delta k \tag{1a}$$

where

$$\Delta k = 2n_p\omega_p/c - n_s\omega_s/c - n_a\omega_a/c \tag{1b}$$

and

$$2\pi\Omega c = \omega_p - \omega_s = \omega_a - \omega_p. \tag{1c}$$

In the above, Δk is the wavevector mismatch of the four interacting waves, the ω's are the circular frequencies of the waves, the n's are their effective refractive indexes, and Ω is the frequency shift of the interaction in units of cm^{-1}.

In an optical fiber, the effective refractive indexes of the waves (hence, also Δk) is determined by two factors. The first is the dispersion of the bulk medium of which the guide is made; the second is the dispersive characteristic of the waveguide itself. We denote the material and waveguide contributions to Δk as Δk_m and Δk_w, respectively, such that $\Delta k = \Delta k_m + \Delta k_w$.

In Fig. 1, curve m shows the dependence of Δk_m upon Ω for fused silica [14], assuming a pump wavelength of 532 nm. A good approximation [5] is

$$\Delta k_m = 2\pi\lambda D(\lambda)\,\Omega^2 \tag{2}$$

where $D(\lambda)$ is the group-velocity dispersion for the medium; $D(\lambda) = \lambda^2(d^2n/d\lambda^2)$. The validity of (2) breaks down when $D(\lambda)$ becomes small (such as near 1.3 μm for fused silica).

A. Phasematching Using Fiber Modes

Phasematching of parametric interactions involving large frequency shifts can be accomplished with various combinations of the waveguide modes of a multimode fiber. The idea is to choose modes for the pump, Stokes, and anti-Stokes waves such that $\Delta k_w = -\Delta k_m$.

One such combination is illustrated in Fig. 2(a) where both pump photons propagate in the LP_{01} mode and both Stokes and anti-Stokes are in the LP_{11} mode [15]. The waveguide contribution is plotted versus Ω in Fig. 1 as curve w_{a1}. This combination of modes is particularly simple to deal with since the curve is almost a horizontal line. Phasematching occurs at the frequency where the contributions from material index dispersion and waveguide modes cross. This combination of modes has been observed in large-frequency shift stimulated parametric mixing [7].

Many possible combinations of modes are possible for achieving phasematching. Typical curves are illustrated by the lines w_{a2} and w_{a3} in Fig. 1. Depending on the particular mode combination, the curves can deviate in either direction from a horizontal line. For estimating frequency shifts and relative positions of different processes it is often sufficient to approximate all such curves with horizontal lines and thus calculate only the wavevector difference at $\Omega = 0$. Many different combinations of modes have been seen in low-power mixing experiments [2]. Typically, Ω is in the range of 1000-2000 cm^{-1} and l_c ranges from 10-50 cm for a pump wavelength in the green.

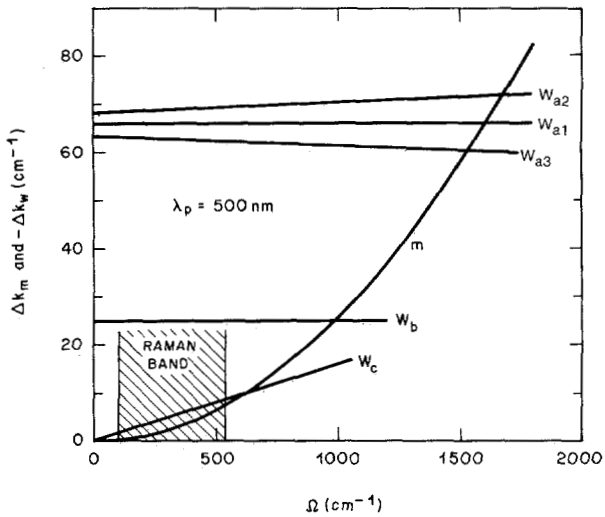

Fig. 1. Phasematching curves for parametric four-photon processes in silica multimode fibers. Curve m is the contribution from material dispersion alone plotted as Δk_m versus frequency shift Ω for a pump wavelength of 500 nm. The contributions from combinations of waveguide modes are plotted as $-\Delta k_w$ for three general types of mode combinations which are illustrated in Fig. 2. Curves w_a are the most general large frequency-shift combinations, curve w_b corresponds to birefringence matching and curve w_c is a divided pump process.

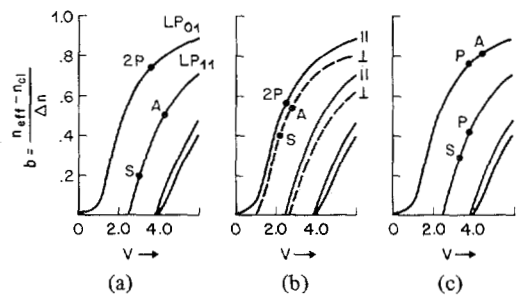

Fig. 2. Three representative combinations of modes for phasematching. These curves do not contain material dispersion. The parameter b is a normalized effective refractive index and the characteristic number V is a normalized frequency [15]. (a) Large frequency shift process; (b) birefringence matching; (c) divided-pump process.

B. Birefringence Matching

Stimulated parametric emission has been observed in a single-mode polarization-preserving fiber by utilizing the fiber birefringence for phasematching [3]. Here the polarizations of the generated waves are perpendicular to the pump polarization and the perpendicular component of the third order susceptibility applies. This process is illustrated in Fig. 2(b) and is similar to that of Fig. 2(a) except now the phasematching comes from the splitting between the $\|$ and $\perp$ components of the fundamental mode rather than the difference between the LP_{01} and LP_{11} modes. This process also results in a horizontal line on the phase matching curves in Fig. 1(curve w_b).

The parametric gain of the birefringence matched interaction is reduced with respect to other mode combinations because the perpendicular susceptibility is only about a third of the parallel susceptibility [16]. Most of this loss is recovered, however, since the overlap integral is about a factor of two larger with all waves in the fundamental mode compared to combinations with different modes. Frequency shifts for birefringence matched parametric emission are typically 100-1000 cm^{-1} and l_c is about 1-2 m.

C. Divided Pump Process

The most commonly observed stimulated parametric process occurs with the pump power divided between the same two modes as the Stokes and anti-Stokes waves [8]-[10]. Such a combination of modes is illustrated in Fig. 2(c). Here there is no wavevector difference at $\Omega = 0$ and the phasematching curve is that of curve w_c in Fig. 1. As will be discussed later, these processes are particularly interesting because of their long coherence lengths. Characteristic values for l_c are usually around 10 m. Frequency shifts are usually between 100 cm^{-1} and 500 cm^{-1}; in this range Raman gain in silica is also important, as shown by the shaded region in Fig. 1 [1], [17], [18]. The presence of Raman gain is a complicating factor which decreases the anti-Stokes generation and increases the Stokes output power although the net gain is not very different.

D. Phasematching Near the Zero Dispersion Wavelength

Stimulated parametric mixing has been observed in long single-mode fibers using pump wavelengths close to the zero-dispersion wavelength [4]. In this region $D(\lambda) \approx 0$ and (2) does not hold because of the importance of higher order terms in the expansion of refractive index versus wavelength. By choosing a pump wavelength slightly longer than the zero dispersion wavelength, phasematching can be achieved over a broad range of frequency shifts.

In the context of the present work the existence of such intrinsically phasematched processes serves as a convenient excuse for simplifying much of the theory to the simplest case where all waves propagate in the fundamental mode with the same linear polarization.

E. Small Frequency Shifts

The coherence length can be quite long if Ω is small. For example, $l_{coh} \approx 2$ km for $\Omega = 1$ cm^{-1} at a 500 nm pump wavelength. In the infrared, where $D(\lambda)$ is smaller, l_{coh} is even longer. Because of these long coherence lengths there is no need for additional phasematching of processes characterized by frequency shifts less than a few cm^{-1}. These would include mixing with Brillouin shifted light [6], mixing of the longitudinal laser modes [5], and self-phase modulation [19].

III. Parametric Gain in a Fiber

A. Coupled Wave Equations

As shown in Appendix A, Maxwell's equations in an optical fiber with a third-order nonlinearity $\chi_3(\Omega)$ take the form of the following coupled wave equations:

$$\frac{dF_s}{dz} = ic_s\chi_3(\Omega)PF_s + ic_4\chi_3(\Omega)PF_a^* e^{i(\Delta k + 2\delta k_p)z}$$

$$\frac{dF_a^*}{dz} = -ic_a\chi_3(\Omega)PF_a^* - ic_4\chi_3(\Omega)PF_s e^{-i(\Delta k + 2\delta k_p)z} \quad (3)$$

where s, a, and p refer to the Stokes, anti-Stokes, and pump waves, respectively, and we assume negligible pump depletion. The quantity F is analogous to the electric field in the plane

wave treatment and is defined such that the power in a given mode at a given wavelength is $|F|^2$. P is the pump power and δk_p is a shift in the pump wave vector arising from the intensity dependent refractive index at the pump frequency. δk_p is proportional to pump power and is defined in (A12) and (A15). Constants c_s, c_a, c_4 contain overlap integrals which are proportional to inverse area and are in general not the same for each term.

The derivation of (3) is outlined in Appendix A for the case in which the pump power is distributed between two fiber modes which are not necessarily the same as the Stokes and anti-Stokes modes. Similar expressions for gain and amplification have been published by Saissy *et al.* [10]. Both derivations are based on an approach of Bloembergen and Shen [20]. The inclusion of wavevector mismatch Δk allows the calculation of gain and amplification as frequency shift Ω is varied. Ω and Δk are defined in (1) and Δk contains both material and waveguide contributions to the refractive index.

The susceptibility χ_3 is, in general, complex and is represented as $\chi_3 = \chi_3' - i\chi_3''$. Parametric gain comes from χ_3' while from (3) it can be seen that χ_3'' leads to Stokes amplification and anti-Stokes absorption [20]. If the parametric process is negligible because, for example, of large wavevector mismatch, the solutions of (3) describe only nonlinear index and Raman effects. The Raman Stokes gain coefficient is $c_s\chi_3''P$ and the Raman anti-Stokes absorption coefficient is $-c_a\chi_3''P$. In fused silica, χ_3'' has a maximum value of 5.5×10^{-16} ESU at a frequency shift of 440 cm^{-1} [17], [18]. The real part, χ_3' is mostly of electronic origin and has a value of 3.5×10^{-15} ESU for frequency shifts greater than 1000 cm^{-1} [17], [19]. Kramers-Kronig relations couple the real and imaginary parts of χ_3 so the Raman gain leads to structure in χ_3' [17]. Variations in χ_3' can be as large as 20 percent.

In the derivation of (3) we have assumed linearly polarized (LP) modes [15]. In all cases, except birefringence matching, all waves propagate with the same linear polarization. This is, of course, much simpler than the general case of arbitrary polarizations for all modes. However, birefringent multimode fibers can preserve linear polarization [21] and should be the most suitable fibers for phasematched parametric interactions.

B. Parametric Gain

In order to bring out the essential features of the parametric gain as a function of Δk we restrict the treatment to the case where both pump waves propagate in the same mode of the fiber, neglect the differences in ω_i and n_i in the coefficients c_i of (3) and choose $\chi_3'' = 0$.

If we assume χ_3 is real rather than complex, the first terms on the right side of (3) give rise to an intensity dependent refractive index and the second terms lead to parametric gain. Let us consider this case in detail. Considerable simplification results when the intensity dependence of the various wavevectors is made explicit. This can be accomplished with the substitutions

$$F_s = G_s e^{i\delta k_s z}; \quad \delta k_s = c_s\chi_3 P$$
$$F_a = G_a e^{i\delta k_a z}; \quad \delta k_a = c_a\chi_3 P. \tag{4}$$

The coupled wave equations (3) become

$$\frac{dG_s}{dz} = ic_4\chi_3 PG_a^* e^{i\kappa z}$$
$$\frac{dG_a^*}{dz} = -ic_4\chi_3 PG_s e^{-i\kappa z} \tag{5}$$

where

$$\kappa = \Delta k - \delta k_s - \delta k_a + 2\delta k_p. \tag{6}$$

For completeness, we write down the general solution for G_s (the solution for G_a^* is similar)

$$G_s = [Ae^{gz} + Be^{-gz}]\, e^{i\kappa z/2} \tag{7}$$

The coefficients of (7) and general expressions for amplification are given in Appendix C. The quantity of primary interest here is g, the Stokes and anti-Stokes exponential gain constant which is

$$g = [(c_4\chi_3 P)^2 - (\kappa/2)^2]^{1/2}. \tag{8}$$

The gain coefficient g is plotted as a function of κ and of Δk in Figs. 3(a) and 3(b) respectively. First consider the dependence on κ. The peak value of g is $c_4\chi_3 P$ and occurs at $\kappa = 0$. The bandwidth of the interaction (the range of κ over which $g > 0$) depends on the pump power and it increases as P increases. This phenomenon also occurs in three photon parametric amplifiers [22] and arises because the Stokes and anti-Stokes power, generated earlier in the fiber, which would be reabsorbed into the pump because of the phase shifts, is more than offset by conversion of pump to Stokes and anti-Stokes power due to the exponential gain.

As shown by Fig. 3(b), an actual experimental measurement of gain versus mismatch will not only measure an increased bandwidth with pump power but also a shift of the peak gain due to the intensity dependent refractive index as can be seen from (6) and (8). By the transformation of (6) we have separated the calculations of the gain spectrum and the shift of the peak gain. The actual shift depends on the particular modes involved in the interaction.

If we choose the simplest case of intrinsic phase matching near the zero dispersion wavelength where pump, Stokes, and anti-Stokes waves all propagate in the fundamental mode with the same polarization, then $\delta k_s = \delta k_a = 2\delta k_p = 2c_4\chi_3 P$. The shift in the gain maximum corresponds to $\Delta k = 2c_4\chi_3 P$. Note that $g = 0$ at $\kappa = \pm 2c_4\chi_3 P$, so the shift approximately equals the bandwidth of the gain curve.

The intensity dependent shift in the gain maximum should lead to interesting time dependent effects for pump pulses as opposed to a CW pump. In extreme cases it might be possible to shift in and out of phasematching during the pulse. Also, the effective phasematching frequency will change when pump depletion occurs.

An alternative approach in dealing with the coupled wave equations of (3) is to neglect the intensity dependent index at the pump wavelength and solve for the value of Δk which gives the maximum gain. This was done in [20] and in computer calculations of [10]. The results for peak gain and bandwidth are unchanged but neglecting δk_p results in a shift of the peak gain which is a factor of two too large.

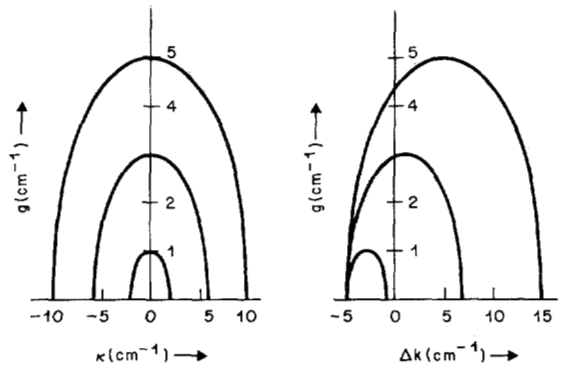

Fig. 3. Gain g from (8) versus phase mismatch parameters κ and Δk as defined in (1b) and (6). The gain is calculated for three values of pump power P such that $c_4\chi_3 P$ equals 1.0, 3.0, and 5.0 cm^{-1}. The shift due to the intensity dependent index depends on overlap integrals and, for the combination of modes illustrated in Fig. 2(a) can be near zero. In the figure, the shift was arbitrarily chosen to be: $\delta\kappa_s + \delta\kappa_a - 2\delta\kappa_p = 5.0$.

IV. Bandwidth

A. Parametric Gain Bandwidth

Bandwidth can be defined from the measured output power versus frequency shift of either the amplified wave or the generated idler.

The general expressions for the Stokes and anti-Stokes powers generated in a fiber of length l can be obtained from (5) and (7) and the coefficients from Appendix C. The powers are $P_s = F_sF_s^* = G_sG_s^*$ and $P_a = F_aF_a^* = G_aG_a^*$ and we continue to take χ_3 to be real. We consider the case where the input signal P_{so} is nonzero while $P_{ao} = 0$. If both P_{so} and P_{ao} are present, interference occurs as is discussed in Appendix C. For $P_{ao} = 0$, the output powers become

$$\frac{P_s}{P_{so}} = 1 + \frac{(c_4\chi_3 Pl)^2}{4}\,\frac{\sinh^2 gl}{(gl)^2} \tag{9a}$$

$$\frac{P_a}{P_{so}} = \frac{(c_4\chi_3 Pl)^2}{4}\,\frac{\sinh^2 gl}{(gl)^2}\,. \tag{9b}$$

Equation (9a) corresponds to Stokes amplification while (9b) represents the anti-Stokes power generated by mixing pump and Stokes waves.

In the limit of large amplification where $gl \gg 1$ the peak output at $\kappa = 0$ reduces to $P_s = P_a = \frac{1}{4}\,P_{so}e^{2gl}$. Equivalent expressions are obtained if the initial signal is P_{ao}. The limit $c_4\chi_3 P \ll \kappa$ corresponds to a mixing experiment where $P_a \ll P_s \ll P$ and P is the pump power. In this limit, (9b) becomes

$$P_a = \frac{P_{so}P^2 l^2 c_4^2\chi_3^2}{4}\,\frac{\sin^2(\kappa l/2)}{(\kappa l/2)^2}\,. \tag{10}$$

From (10), a convenient definition of the mixing bandwidth is

$$\Delta\kappa_B = \frac{2\pi}{l} \tag{11}$$

which is slightly greater than full-width-half-maximum. Equation (11) shows that the bandwidth should become narrower with increasing fiber length. In actual experiments, the ideal $\sin^2(x)/x^2$ bandwidth is obtained only with short fibers; in long fibers the bandwidth is broadened from variations in phasematching frequency along the fiber. The result is to impose an effective coherence length due to fiber imperfections.

A general expression for bandwidth which reduces to (11) at low power is

$$\Delta\kappa_B = 2\left[\left(\frac{\pi}{l}\right)^2 + (c_4\chi_3 P)^2\right]^{1/2} \tag{12}$$

At high power, $\Delta\kappa_B$ is proportional to P and is independent of fiber length l. At low power $\Delta\kappa_B$ reduces to the bandwidth measured by a low power mixing experiment in a perfect fiber and it varies inversely with length.

The frequency bandwidth $\Delta\Omega_B$ is related to $\Delta\kappa_B$ by

$$\Delta\Omega_B = \Delta\kappa_B \left.\frac{d\Omega}{d(\Delta k)}\right|_{\Delta k=0} \tag{13}$$

The value of $d\Omega/d(\Delta k)$ can be obtained from phasematching curves of the type shown in Fig. 1. For high pump power the parametric bandwidth is thus

$$\Delta\Omega_B = 2c_4\chi_3 P \left.\frac{d\Omega}{d(\Delta k)}\right|_{\Delta k=0} \tag{14}$$

B. Pump Linewidth

The pump linewidth is not constant along the fiber but increases due to self-phase modulation [19]. The frequency broadening from self-phase modulation δv_{spm} is proportional to the initial pump bandwidth and the intensity dependent refractive index at the pump frequency. In the present notation it can be expressed as

$$\delta v_{spm} = \delta v_p \cdot c_4\chi_3 Pl \tag{15}$$

where P is the peak power of the pump pulse. For large $c_4\chi_3 Pl$, δv_{spm} can be much larger than the input linewidth. Equation (15) holds only for transform limited pulses although here we also apply it to more general pump pulses. This is justified by somewhat qualitative arguments based on the structure of nontransform-limited pulses [23].

C. Relation of Gain to Pump Linewidth and Parametric Bandwidth

To calculate the peak gain using pump pulses, one usually uses the peak pump power in (8). This is valid only if signal and pump pulses do not separate due to group-velocity dispersion and if the pump linewidth is less than the parametric gain bandwidth.

If the pump linewidth is broader than the gain bandwidth, the effective gain is reduced. The situation is quite similar to transient Raman gain where maximum gain occurs only if the pump linewidth is less than the Raman gain bandwidth [24]. This relation between pump linewidth and gain bandwidth is an essential feature of the explanation of the characteristic length l_c found with stimulated parametric emission.

To see the relation between parametric gain and bandwidth we choose the simple case of two pump frequencies v_1 and v_2 with equal amplitudes $F_1(v_1) = F_2(v_2)$ (v is in the same units as Ω.) The total pump power varies with time as

$$P = 2P_1\,[1 + \cos 2\pi c(v_1 - v_2)\,t]\,. \tag{16}$$

If v_1-v_2 is small, the gain from (8) will vary between $g_{max} = 4c_4\chi_3 P_1$ and zero. In the absence of large intensity dependent shifts in the phasematching frequency the average gain will be $2c_4\chi_3 P_1$ with $P_{av} = 2P_1$. If these two pump frequencies are widely separated, there will be three different phasematched interactions as illustrated in Fig. 4(a). The gain measured with a tunable signal would show three peaks corresponding to v_1 alone, the combination of v_1 and v_2, and v_2 alone. The frequency shifts are labeled Ω_1, Ω_2, and Ω_3. With $F_1 = F_2$, then $g_1 = g_3 = c_4\chi_3 P_1$ and $g_2 = 2c_4\chi_3 P_1$. The gain at Ω_2 is the same as if all the pump power had been at a single frequency and is half the peak gain using the peak power from (16).

The two different gain curves shown in Fig. 4 correspond to the limits where v_1-v_2 is less or greater than $\Delta\Omega_B$ where $\Delta\Omega_B$ is the parametric gain bandwidth as defined in (12) and (13). The limit v_1-$v_2 \ll \Delta\Omega_B$ is illustrated schematically in Fig. 4(b) where it is clear that all three interactions can contribute to the gain. Adding the three contributions gives the same maximum gain as was obtained using the maximum power from (16). The combination gain will vary in time with frequency v_1-v_2 because the various contributions can either add or subtract as their relative phases change. These beating effects can be derived with the formalism of Appendix A by retaining those terms in the expansions (A7) which have essentially the same wavevector but whose frequencies differ slightly from the Stokes and anti-Stokes frequencies.

For the particularly useful case of a mode-locked pump pulse train which involves a large number of modes N, the peak power is $\sim NP_{av}$. Extending the previous arguments to N frequencies, the maximum gain for $\delta v_p \ll \Delta\Omega_B$ is proportional to NP_{av} while for $\delta v_p \gg \Delta\Omega_B$ the maximum gain is proportional to P_{av}. For the present work, the essential result is that there will be a significant drop in peak parametric gain once $\delta v_p \approx \Delta\Omega_B$.

V. Calculation of l_c

Stimulated emission occurs with a threshold [25] about $2gl = 16$ which is clearly the high power limit for both the parametric bandwidth and the pump broadening. Thus, we can use (14) and (15) to calculate the fiber length l_E where the pump and gain bandwidths are equal.

The result is

$$l_E = \frac{2}{\delta v_p} \left.\frac{d\Omega}{d(\Delta k)}\right|_{\Delta k=0} \tag{17}$$

which does not require knowledge of either the intensity dependent gain bandwidth or self phase modulation.

The practical useful length is greater than l_E and is determined by the onset of competing processes which, although of lower gain, are not as sensitive to length. The competing process is usually stimulated Raman scattering which, depending on the particular phasematched process and on overlap integrals, has about $\frac{2}{3}$ the gain of the parametric process. Ideally, the total amplification for the two competing processes should be compared but this is hardly necessary for most purposes where one is interested in deciding on a fiber length of 1 or 10 m rather than distinctions of a few cm.

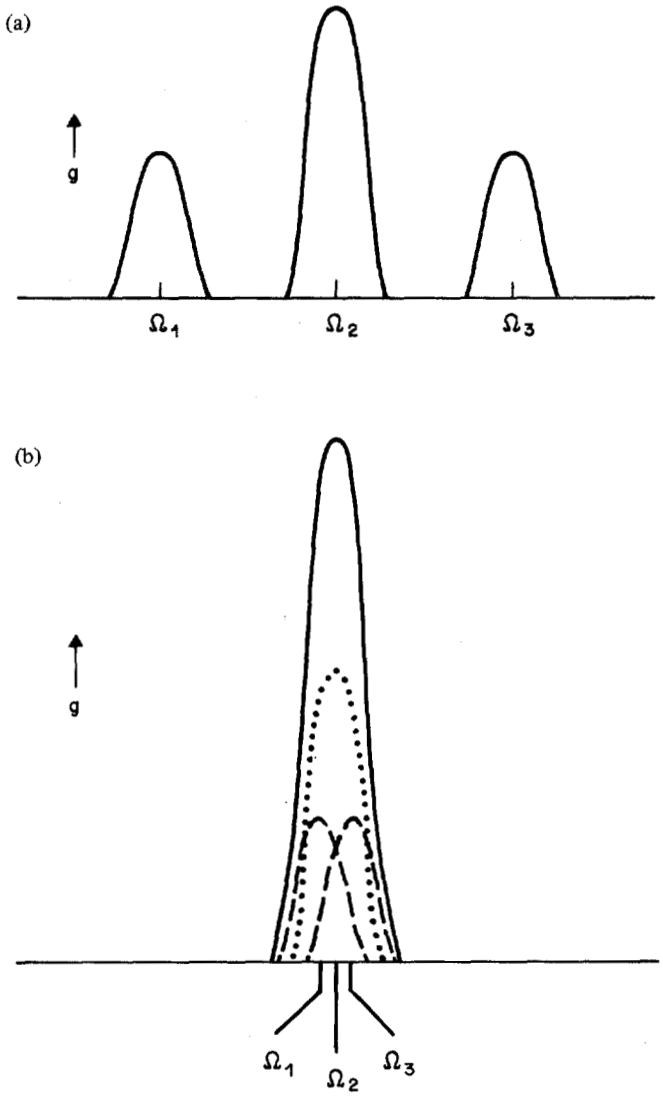

Fig. 4. Gain as measured with a tunable narrow line signal for two pump frequencies v_1 and v_2 in two limits. (a) The two pump frequencies are separated by more than the gain bandwidth of the parametric process; frequency shifts Ω_1, Ω_2, Ω_3 correspond to phasematched interactions with $2v_1$, $v_1 + v_2$ and $2v_2$, respectively. (b) The two pump frequencies are separated by much less than the gain bandwidth.

A useful rule of thumb for choosing a fiber length is that length which matches the low-power parametric mixing bandwidth to the initial pump linewidth leading to

$$l_c = \frac{2\pi}{\delta v_p} \left.\frac{d\Omega}{d(\Delta k)}\right|_{\Delta k=0} \tag{18}$$

where δv and Ω are in units of cm^{-1}. For this length both stimulated parametric emission and stimulated Raman scattering will appear. Longer lengths favor stimulated Raman scattering and shorter lengths favor parametric output.

To illustrate the calculation of l_c we choose examples from the published literature.

First consider mode combinations for which the waveguide contribution to the phasematching curve (Fig. 1) is a horizontal line which gives

$$\left.\frac{d\Omega}{d(\Delta k)}\right|_{\Delta k=0} = (4\pi\lambda D(\lambda)\,\Omega_{pm})^{-1} \tag{19}$$

where Ω_{pm} is the phasematched frequency shift and we have used the quadratic dependence of the material dispersion from (2). As a first example we consider processes with large frequency shifts which have recently been reported [7], [13]. Measured shifts were approximately 2400 cm^{-1} with a 532 nm pump [7] and 2800 cm^{-1} with a 1.06 μm pump [13]. While the exact frequency shift depends on detailed characteristics of the fibers, it is straightforward to estimate l_c from (18) and (19) and the measured frequency shift. At 532 nm $D(\lambda) = 0.066$ and at 1.06 μm $D(\lambda) = 0.012$ [26]. We estimate pump linewidths to be 1 cm^{-1} and 0.5 cm^{-1}, respectively. For these frequency shifts l_c is 59 cm at 532 nm and 280 cm at 1.06 μm. Note that for our definition of l_c both stimulated parametric and Raman outputs should be observed. Shorter fibers must be used to eliminate stimulated Raman scattering. A second example is a birefringence matched process [3] with a 532 nm pump wavelength, a 1 cm^{-1} pump bandwidth, and a 1000 cm^{-1} frequency shift, $d\Omega/d(\Delta k) = 22.7$ and $l_c = 142$ cm. This is in good agreement with experimental results [3].

A second class of mode combinations is illustrated by the divided pump process [w_c in Fig. 1 and Fig. 2(c)] for which $\Delta k_w \sim \Omega$. Thus

$$\left.\frac{d\Omega}{d(\Delta k)}\right|_{\Delta k=0} = (2\pi\lambda D(\lambda)\,\Omega_{pm})^{-1}. \tag{20}$$

With a 532 nm pump and $\Omega = 400$ cm^{-1} l_c is 7 m. This is in agreement with previous results [8]. It can be seen that a factor of two of this large l_c comes from the better match of slopes of waveguide and material contributions to Δk. Most of the increase, however, arises because the frequency shift Ω is relatively small.

VI. Conclusion

We have shown that there is a characteristic length for four-photon parametric interactions in optical fibers; for fibers longer than the characteristic length, the gain per unit length decreases. This length is related to the pump linewidth and frequency bandwidth of the parametric interaction which can be calculated from phasematching curves containing separate contributions from material and waveguide index dispersion.

The characteristic length increases for small frequency shifts and for pump frequencies near the point of minimum group velocity dispersion. Furthermore, the length increases with a better match between the slopes of the material and waveguide contributions of the total phase mismatch. This result suggests that selection of fiber index profiles which modify the relative slopes of the index dispersion curves for various modes could result in extremely long useful fiber lengths.

Starting with coupled wave equations, general expressions for CW amplification were obtained. These expressions also apply to optical pulses if the pump linewidth is much less than the parametric gain bandwidth. It was shown that the gain bandwidth is intensity dependent and that the intensity dependent refractive index shifts the phasematching frequency. At high and low pump power, limiting forms of the expression for amplification apply to stimulated emission and to mixing.

The coupled wave equations in a fiber were shown to be of the same form as the planewave equations but modified by constant factors related to an integral over the mode fields. This is a general property of nonlinear interactions in fibers which applies not only to the parametric interaction but also to stimulated Raman and Brillouin scattering, self-phase modulation, and optical Kerr effect. In all these cases the procedure is to use the planewave equations but to modify the coupling coefficient with the overlap integral which serves as an effective fiber core area.

Appendix A
Derivation of Coupled Wave Equations

In this section the derivation of the general coupled wave equations in a fiber is outlined. The coupled wave equations are the same as those describing the nonlinear interaction between uniform planewaves except for constant factors which describe the strength of the coupling between the various waveguide modes. These factors are called overlap integrals which are equivalent to the inverse of an effective area of the fiber core and are discussed further in Appendix B.

The wave equations in the presence of the third-order nonlinearity χ_3 follow:

$$\nabla^2\vec{E}(z,r,\theta) - \frac{n^2}{c^2}\frac{\partial^2}{\partial t^2}\vec{E}(z,r,\theta) = \frac{4\pi(4\chi_3)}{c^2}\frac{\partial^2\vec{E}^3(z,r,\theta)}{\partial t^2} \tag{A1}$$

where the factor of 4 in the definition of χ_3 follows the convention of Minck, *et al.* [27], n is the refractive index, and c is the speed of light. The dielectric medium is considered to be lossless. The electric field is expanded in frequency and in terms of the waveguide transverse modes. In doing this it is assumed that the modes which are solutions of the transverse part of the wave equation are not perturbed by the presence of the nonlinear polarization. The z axis is taken to be the axis of the fiber. The electric field is thus

$$\vec{E}(z,r,\theta,t) = \sum_{l,m}\vec{A}_{lm}(z)\,\psi_m(r,\theta)\cos(k_{lm}z - \omega_l t + \phi_{lm}) \tag{A2}$$

where l refers to the frequency, m the mode number, k_{lm} the wavevector, and ϕ_{lm} the phase. The power propagating in the mth mode at frequency ω_l is

$$P_{lm} = |\vec{A}_{lm}(z)|^2 N_{lm}^2 \tag{A3}$$

where we define

$$N_{lm}^2 = \frac{cn_{lm}}{8\pi}\int_0^\infty\int_0^{2\pi}\psi_m^2(r,\theta)\,r\,dr\,d\theta \tag{A4}$$

and $n_{lm} = ck_{lm}/\omega_l$ is the effective refractive index of mode m at ω_l. There is considerable convenience in dealing with quantities which can be easily related to the power in a given mode so we define a new amplitude

$$|\vec{F}_{lm}(z)| \equiv N_{lm} |\vec{A}_{lm}(z)|. \tag{A5}$$

From (A3), we have $P_{lm} = |\vec{F}_{lm}(z)|^2$.

The energy flow at the pump, Stokes, and anti-Stokes frequencies can, in general, be distributed over all the modes of the fiber. With little loss of generality, however, and a great gain in simplicity we restrict our attention to situations in which only a small number of modes are involved. In particular, we allow the pump power to be in either or both of two modes which we label 1 and 2. The Stokes and anti-Stokes powers are limited to single modes labeled s and a, respectively. We further restrict our attention to the situation in which the pump powers are much greater than P_s or P_a so that depletion of the pump is negligible. The frequency index l and the mode index m can then be replaced by a single index m.

Following the usual procedure we take

$$\vec{A}_m(z)\cos(k_m z - \omega_m + \phi_m) = \frac{\vec{F}_m(z)}{2N_m} e^{i(k_m z - \omega_m t)} + \frac{\vec{F}_m^*(z)}{2N_m} e^{-i(k_m z - \omega_m t)}. \tag{A6}$$

Coupled wave equations are obtained by collecting terms of the same frequency and by using the slowly varying envelope approximation in which we assume $d^2F/dz^2 \ll ik\, dF/dz$.

To account for mode coupling, the resulting equations are multiplied by the appropriate $\psi_m(r,\theta)$, integrated over the waveguide cross section, and divided by $\int\int \psi_m^2\, r dr d\theta$. This, along with the definition of N_m in (A4) gives the overlap integral which we represent as $\langle s12a\rangle$. A general expression for the integral and a brief discussion of its application to various nonlinear processes is given in Appendix B.

There will be parametric interactions where phasematching occurs with pump light divided between two fiber modes and other parametric interactions where phasematching is achieved with all the pump light in a single mode. For the most general case in which pump power is divided unequally between modes 1 and 2 and Stokes and anti-Stokes light propagates in two different modes s and a

$$\begin{aligned}
\frac{dF_s}{dz} &= ic_{s1}\chi_3(\Omega) F_1 F_1^* F_s + ic_{s2}\chi_3(\Omega) F_2 F_2^* F_s \\
&\quad + ic_{s3}\chi_3(\Omega) F_1 F_2 F_a^* e^{i\Delta kz} \\
\frac{dF_a^*}{dz} &= -ic_{a1}\chi_3(\Omega) F_1 F_1^* F_a^* - ic_{a2}\chi_3(\Omega) F_2 F_2^* F_a^* \\
&\quad - ic_{a3}\chi_3(\Omega) F_1^* F_2^* F_s e^{-i\Delta kz} \\
\frac{dF_1}{dz} &= ic_{11}\chi_3(0) F_1 F_1^* F_1 + ic_{12}\chi_3(0) F_2 F_2^* F_1 \equiv i\delta k_1 F_1 \\
\frac{dF_2}{dz} &= ic_{21}\chi_3(0) F_1 F_1^* F_2 + ic_{22}\chi_3(0) F_2 F_2^* F_2 \equiv i\delta k_2 F_2.
\end{aligned} \tag{A7}$$

Here, $2\pi c\Omega = \omega_p - \omega_s = \omega_a - \omega_p$ and $\Delta k = (n_1 + n_2)\,\omega_p/c - n_s\omega_s/c - n_a\omega_a/c$.

The coefficients of (A7) are

$$\begin{aligned}
c_{s1} &= \frac{96\pi^2\omega_s}{n_s^2c^2}\langle s11s\rangle; \quad c_{s2} = \frac{96\pi^2\omega_s}{n_s^2c^2}\langle s22s\rangle \\
c_{a1} &= \frac{96\pi^2\omega_a}{n_a^2c^2}\langle a11a\rangle; \quad c_{a2} = \frac{96\pi^2\omega_a}{n_a^2c^2}\langle a22a\rangle \\
c_{11} &= \frac{48\pi^2\omega_p}{n_1^2c^2}\langle 1111\rangle; \quad c_{12} = \frac{96\pi^2\omega_p}{n_1^2c^2}\langle 1221\rangle \\
c_{21} &= \frac{96\pi^2\omega_p}{n_2^2c^2}\langle 2112\rangle; \quad c_{22} = \frac{48\pi^2\omega_p}{n_2^2c^2}\langle 2222\rangle \\
c_{s3} &= \frac{96\pi^2\omega_s}{n_s^2c^2}\langle s12a\rangle; \quad c_{a3} = \frac{96\pi^2\omega_a}{n_a^2c^2}\langle a12s\rangle.
\end{aligned} \tag{A8}$$

The third-order susceptibility is, in general, complex with $\chi_3(\Omega) = \chi_3'(\Omega) - i\chi_3''(\Omega)$. In (A7) δk_1 and δk_2 are intensity dependent contributions to the wavevector at the pump frequency. Here $\chi_3(0)$ is real from the general condition that $\chi_3^*(-\Omega) = \chi_3(\Omega)$ [20] so $F_1(z) = F_1(0)\exp(\delta k_1 z + \phi_1)$ and $F_2(z) = F_2(0)\exp(\delta k_2 z + \phi_2)$.

We can use this result for $F_1(z)$ and $F_2(z)$ to combine (A7) into a simpler form of the Stokes and anti-Stokes coupled wave equations.

$$\begin{aligned}
\frac{dF_s}{dz} &= ic_s\chi_3(\Omega) PF_s + ic_4\chi_3(\Omega) PF_a^* e^{i(\Delta k + 2\delta k_p)z} \\
\frac{dF_a^*}{dz} &= -ic_a\chi_3(\Omega) PF_a^* - ic_4\chi_3(\Omega) PF_s e^{-i(\Delta k + 2\delta k_p)z}.
\end{aligned} \tag{A9}$$

Here we have used $|F_1|^2 = P_1$, $|F_2|^2 = P_2$ and defined the total pump power $P = P_1 + P_2$. The initial phases of the pump waves ϕ_1 and ϕ_2 are arbitrarily taken to be zero but there are no restrictions on the phases of the Stokes and anti-Stokes waves ϕ_s and ϕ_a. $\chi(\Omega)$ can be complex. For simplicity we neglect the differences in ω_i/n_i^2 and define the quantity

$$Q \equiv \frac{48\pi^2\omega_p}{n^2c^2}. \tag{A10}$$

The various n_{lm} are replaced by an average refractive index n. With this approximation

$$c_{s3} \approx c_{a3} \equiv c_3. \tag{A11}$$

The coefficients of (A9) become

$$\begin{aligned}
c_s &= c_{s1}\frac{P_1}{P} + c_{s2}\frac{P_2}{P} = \frac{2Q}{P}(P_1\langle s11s\rangle + P_2\langle s22s\rangle) \\
c_a &= c_{a1}\frac{P_1}{P} + c_{a2}\frac{P_2}{P} = \frac{2Q}{P}(P_1\langle a11a\rangle + P_2\langle a22a\rangle) \\
c_4 &= c_3\frac{2}{P}\sqrt{P_1P_2} = \frac{2Q}{P}\sqrt{P_1P_2}\,\langle s12a\rangle \\
\delta k_p &= (\delta k_1 + \delta k_2)/2 = \frac{QP_1}{2}(\langle 1111\rangle + 2\langle 2112\rangle) \\
&\quad + \frac{QP_2}{2}(\langle 2222\rangle + 2\langle 1221\rangle).
\end{aligned} \tag{A12}$$

The expression for c_4 can be further simplified by defining a parameter γ which expresses the division of pump power between modes 1 and 2

$$p_1 = P\frac{(1+\gamma)}{2};\quad p_2 = P\frac{(1-\gamma)}{2} \tag{A13}$$

$$c_4 = Q\langle s12a\rangle\sqrt{1-\gamma^2} \tag{A14}$$

γ varies between +1 and −1 with maximum gain at $\gamma = 0$ corresponding to equal power in the two pump modes.

Equation (A9) also applies to the case where all the pump power is confined to one fiber mode p with the coefficients

$$\begin{aligned} c_s &= 2Q\langle spps\rangle \\ c_a &= 2Q\langle appa\rangle \\ c_4 &= Q\langle sppa\rangle \\ \delta k_p &= Q\langle pppp\rangle. \end{aligned} \tag{A15}$$

Note that c_s, c_a, and c_4 of (A15) can be obtained by taking $P_1 = P_2 = P/2$ in (A12). There, however, are differences in the intensity dependent index at the pump frequency.

Appendix B
Overlap Integrals

The overlap integrals arising from integration over the waveguide-mode fields are equivalent to a fiber inverse core area and can differ depending on the specific modes involved. *The overlap integrals all have the same form for all nonlinear effects characterized by the same order of nonlinearity.* For example, four-photon parametric mixing, stimulated Raman scattering, self-phase modulation, and the optical Kerr effect all arise from the third order nonlinearity and are characterized by the same type of overlap integral.

We define the overlap integral as

$$\langle s12a\rangle = \frac{\int_0^{2\pi}\int_0^{\infty}\psi_s\psi_1\psi_2\psi_a\, r dr d\theta}{D_s^{1/2}D_1^{1/2}D_2^{1/2}D_a^{1/2}}$$

$$D_m = \int_0^{2\pi}\int_0^{\infty}\psi_m^2\, r dr d\theta. \tag{B1}$$

With this definition it is not necessary to choose any particular normalization for the mode functions ψ_m. The overlap integrals have units of (area)$^{-1}$ so that $P\langle s12a\rangle$ represents an effective intensity. Depending on the particular combination of modes, the effective area provided by the overlap integral can be greater or less than the actual fiber core area. Usually, however, the difference is not more than a factor of two so that the formalism as established in Appendix A provides a straightforward way of estimating nonlinear gains and thresholds in real fibers. This overlap integral is nonzero only for combinations of modes with the proper symmetry.

The same integrals apply to other third order nonlinear processes such as Raman gain and the optical Kerr effect. From (A9) the Raman gain coefficient with pump and Stokes waves in the same mode becomes

$$g_s = 2Q\chi_3''P\langle 1111\rangle \tag{B2}$$

and if the pump and Stokes waves are in different modes

$$g_s = 2Q\chi_3''P\langle 1122\rangle. \tag{B3}$$

Here we have labeled the modes simply by 1 and 2.

The parametric gain corresponding to (B2) where all waves propagate in the same mode is

$$g_4 = Q\chi_3'P\langle 1111\rangle. \tag{B4}$$

The factor of 2 difference in the expressions (B2) and (B4) relating gains to susceptibilities arises because in the expansion of E^3 both EE^* and E^*E contribute to Raman gain (and the nonlinear index) [28].

In the optical Kerr effect [29] one measures the difference in intensity dependent refractive indexes parallel and perpendicular to a strong linearly polarized pump wave. The indexes in turn depend on the parallel and perpendicular components of χ_3'. If both pump and probe waves are in the same mode

$$\delta n_{\parallel} - \delta n_{\perp} = (\delta k_{\parallel} - \delta k_{\perp})\, c/\omega = \frac{2c}{\omega} QP(\chi_{\parallel}' - \chi_{\perp}')\langle 1111\rangle. \tag{B5}$$

If all waves are in the fundamental LP_{01} (or HE_{11}) mode which we approximate with the Gaussian function $\psi_1 = \exp(-r^2/w^2)$, then $\langle 1111\rangle = 1/\pi w^2$. Here, w is the $1/e$ amplitude radius. This radius is approximately the core radius so the effective area for stimulated Raman scattering in a single-mode fiber or for the birefringence matched parametric process can be approximated by the fiber core area. Detailed calculations require the actual mode profile which differs slightly from a Gaussian mode and which could be larger or smaller than the core size depending on wavelength and fiber parameters. The commonly used spot size is based on intensity rather than amplitude and is typically somewhat smaller than the core size.

The effective area is larger if higher order modes are involved. For example, if we approximate the LP_{11} mode by the higher order Gaussian mode $\psi_2 = (1 - 2r^2/w^2)\exp(-r^2/w^2)$, then $\langle 1122\rangle = 1/2\pi w^2$. This overlap integral would apply to the divided pump parametric process where $\psi_1 = \psi_a = LP_{01}$ and $\psi_2 = \psi_s = LP_{11}$. It would also apply to the stimulated parametric emission observed by Lin and Bösch for which $\psi_1 = \psi_p = LP_{01}$ and $\psi_2 = \psi_s = \psi_a = LP_{11}$. The effective area is twice as large with the higher order mode than if all waves are in the fundamental mode. Hence, the argument in Section II-B that gains in the birefringence matched and divided pump parametric processes are nearly the same despite the factor of three difference in susceptibilities.

Appendix C
General Expressions for Amplification

The general solution for G_s and G_a^* of (5) will be

$$\begin{aligned} G_s &= (Ae^{gz} + Be^{-gz})\, e^{i(\kappa/2)z} \\ G_a^* &= (Ce^{gz} + De^{-gz})\, e^{-i(\kappa/2)z} \end{aligned} \tag{C1}$$

where g is from (8) and κ is from (6). The constants A, B, C, D are determined from (C1), the coupled wave equations (5) and the initial condition that at $z = 0$: $F_s = F_{so} = G_{so}$, $F_a^* = F_{ao}^* = G_{ao}^*$. χ_3 is real.

$$A = \frac{[g - i(\kappa/2)]\ G_{so} + ic_4\chi_3(\Omega)PG_{ao}^*}{2g}$$

$$B = \frac{[g + (i\kappa/2)]\ G_{so} - ic_4\chi_3(\Omega)PG_{ao}^*}{2g}$$

$$C = \frac{-ic_4\chi_3(\Omega)PG_{so} + [g + (i\kappa/2)]\ G_{ao}^*}{2g}$$

$$D = \frac{ic_4\chi_3(\Omega)PG_{so} + [g - (i\kappa/2)]\ G_{ao}^*}{2g} \tag{C2}$$

If both P_{so} and P_{ao} are initially present then interference between them will occur and, depending on the relative phases of pump, Stokes, and anti-Stokes waves, the amplification will be either increased or decreased. For $gl \gg 1$ and $\kappa = 0$ which corresponds to the peak of the gain curve the Stokes amplification is

$$P_s = \left[\frac{P_{so}}{4} + \frac{P_{ao}}{4} + \frac{\sqrt{P_{so}P_{ao}}}{2}\cos\left(\phi_s + \phi_a - \frac{\pi}{2}\right)\right]e^{2gl}. \tag{C3}$$

Here $P_s = G_sG_s^*$ and at $\kappa = 0$

$$G_s = \tfrac{1}{2}\,(G_{so} + iG_{ao}^*)\,e^{g_sl}. \tag{C4}$$

The initial phase of the pump wave was set at $\phi_p = 0$ and ϕ_a and ϕ_s are defined as

$$F_{so} = |F_{so}|\,e^{i\phi_s}$$
$$iF_{ao}^* = |F_{ao}|\,e^{i(\pi/2\,-\phi_a)}. \tag{C5}$$

Stokes amplification from (C3) will be a maximum for $\phi_s + \phi_a = \pi/2$ and a minimum for $\phi_s + \phi_a = -\pi/2$.

References

[1] R. H. Stolen, "Fiber Raman lasers," in *Fiber and Integrated Optics*, D. B. Ostrowsky, Ed. New York: Plenum, 1979; *Fiber Integ. Opt.*, vol. 3, pp. 21–51, 1980; K. O. Hill, B. S. Kawasaki, D. C. Johnson, and Y. Fujii, "Nonlinear effects in optical fibers," in *Fiber Optics–Advances in Research and Development*, B. Bendow and S. S. Mitra, Eds. New York: Plenum, 1979.

[2] R. H. Stolen, J. E. Bjorkholm, and A. Ashkin, "Phase-matched three-wave mixing in silica fiber optical waveguides," *Appl. Phys. Lett.*, vol. 24, pp. 308–310, 1974.

[3] R. H. Stolen, M. A. Bösch, and C. Lin, "Phase-matching in birefringent fibers," *Opt. Lett.*, vol. 6, pp. 213–215, 1981.

[4] K. Washio, K. Inoue, and T. Tanigawa, "Efficient generation of near-IR stimulated light scattering in optical fibers pumped in low-dispersion region at 1.3 μm," *Electron. Lett.*, vol. 16, pp. 331–333, 1980; C. Lin, W. A. Reed, and A. D. Pearson, "Phase matching in the minimum-chromatic-dispersion region of single-mode fibers for stimulated four photon mixing," *Opt. Lett.*, vol. 6, pp. 493–495, 1981.

[5] K. O. Hill, D. C. Johnson, B. S. Kawasaki, and R. I. MacDonald, "cw three-wave mixing in single-mode optical fibers," *J. Appl. Phys.*, vol. 49, pp. 5098–5106, 1974.

[6] K. O. Hill, B. S. Kawasaki, and D. C. Johnson, "cw generation of multiple Stokes and anti-Stokes Brillouin shifted frequencies," *Appl. Phys. Lett.*, vol. 29, pp. 185–187, 1976.

[7] C. Lin and M. A. Bösch, "Large-Stokes-shift stimulated four-photon mixing in optical fibers," *Appl. Phys. Lett.*, vol. 38, pp. 479–481, 1981.

[8] R. H. Stolen, "Phase-matched stimulated four-photon mixing in silica-fiber waveguides," *IEEE J. Quantum Electron.*, vol. QE-11, pp. 100–103, 1975.

[9] R. H. Stolen and W. N. Leibolt, "Optical fiber modes using stimulated four-photon mixing," *Appl. Opt.*, vol. 15, pp. 239–243, 1976; C. Lin, R. H. Stolen, and R. K. Jain, "Group velocity matching in optical fibers," *Opt. Lett.*, vol. 1, pp. 205–207, 1977.

[10] A. Säissy, J. Botineau, A. A. Azéma, and F. Gires, "Diffusion Raman stimulée à trois ondes dans une fibre optique," *Appl. Opt.*, vol. 19, pp. 1639–1646, 1980.

[11] J. Botineau, F. Gires, A. Säissy, C. Vannes, and A. Azéma, "Laser Raman à fibre emettant dans un très large domaine spectral," *Appl. Opt.*, vol. 17, pp. 1208–1209, 1978.

[12] Y. Fujii, B. S. Kawasaki, K. O. Hill, and D. C. Johnson, "Sum-frequency light generation in optical fibers," *Opt. Lett.*, vol. 5, pp. 48–50, 1980; K. O. Hill, B. S. Kawasaki, Y. Fujii, and D. C. Johnson, "Efficient sequence-frequency generation in a parametric fiber-optic oscillator," *Appl. Phys. Lett.*, vol. 36, pp. 888–890, 1980.

[13] K. O. Hill, D. C. Johnson, and B. S. Kawasaki, "Efficient conversion of light over a wide spectral range by four-photon mixing in a multimode graded-index fiber," *Appl. Opt.*, vol. 20, pp. 1075–1079, 1981.

[14] Index data for fused SiO_2 from *American Institute of Physics Handbook*. New York: McGraw-Hill, 1963, p. 6.25.

[15] D. Gloge, "Weakly guiding fibers," *Appl. Opt.*, vol. 10, pp. 2252–2258, 1971.

[16] A. Owyoung, Ph.D. dissertation, California Inst. Technol., Clearinghouse for Federal Scientific Tech. Inform. Rep. AFOSR-TR-71-3132, 1971.

[17] R. W. Hellwarth, J. Cherlow, and T. Yang, "Origin and frequency dependence of nonlinear optical susceptibilities of glasses," *Phys. Rev. B*, vol. 11, pp 964–967, 1975; and "Frequency dependence of the nonlinear optical susceptibility of five glasses," in *Laser Induced Damage in Optical Materials*, A. J. Glass and A. H. Guenther, Eds. Washington, DC: Nat. Bur. Stand. Special Pub. 414, pp. 207–209.

[18] R. H. Stolen and E. P. Ippen, "Raman gain in glass optical waveguides," *Appl. Phys. Lett.*, vol. 22, pp. 276–278, 1973.

[19] F. Shimizu, "Frequency broadening in liquids by a short light pulse," *Phys. Rev. Lett.*, vol. 10, pp. 1097–1100, 1967; R. H. Stolen and C. Lin, "Self-phase modulation in silica optical fibers," *Phys. Rev. A*, vol. 17, pp. 1448–1453, 1978.

[20] N. Bloembergen and Y. R. Shen, "Coupling between vibrations and light waves in Raman laser media," *Phys. Rev. Lett.*, vol. 12, pp. 504–507, 1964; Y. R. Shen and N. Bloembergen, "Theory of stimulated Raman and Brillouin scattering," *Phys. Rev.* vol. 137A, pp. 1787–1805, 1965; N. Bloembergen, *Nonlinear Optics*. New York: W. A. Benjamin, 1965.

[21] R. E. Wagner, R. H. Stolen, and W. Pleibel, "Polarization preservation in multimode fibers," *Electron. Lett.*, vol. 17, pp. 177–178, 1981; A. J. Snyder and W. R. Young, "Modes of optical waveguides," *J. Opt. Soc. Amer.*, vol. 68, pp. 297–309, 1978.

[22] R. G. Smith, "Effects of momentum mismatch on parametric gain," *J. Appl. Phys.*, vol. 41, pp. 4121–4124, 1975.

[23] R. H. Stolen, "Nonlinearity in fiber transmission," *Proc. IEEE*, vol. 68, pp. 1232–1236, 1980.

[24] W. Kaiser and M. Maier, "Stimulated Rayleigh, Brillouin and Raman spectroscopy," in *Laser Handbook*, vol. 2, F. T. Arecchi and E. O. Schulz-Dubois Eds. Amsterdam: North Holland, 1972, pp. 1077–1150.

[25] R. G. Smith, "Optical power handling capacity of low loss optical fibers as determined by stimulated Raman and Brillouin scattering," *Appl. Opt.*, vol. 11, pp. 2489–2494, 1972.

[26] D. Gloge, "Dispersion in weakly guiding fibers," *Appl. Opt.*, vol. 10, pp. 2442–2446, 1971. Note that $D(\lambda)$ is related to D as expressed in ps/nm · km by the factor $c\lambda$.

[27] R. W. Minck, R. W. Terhune, and C. C. Wang, "Nonlinear optics," *Appl. Opt.*, vol. 5, pp. 1595–1628, 1966.

[28] P. D. Maker, R. W. Terhune, and O. M. Savage, "Intensity dependent changes in the refractive index of liquids," *Phys. Rev. Lett.*, vol. 12, pp. 507–509, 1964; P. D. Maker and R. W. Ter-

hune, "Study of optical effects due to an induced polarization third order in the electric field strength," *Phys. Rev.*, vol. 137, pp. A801–A818, 1966.
[29] J. M. Dziedzic, R. H. Stolen, and A. Ashkin, "Optical Kerr effect in long fibers," *Appl. Opt.*, vol. 20, pp. 1403–1406, 1981.

Roger H. Stolen was born in Madison, WI, in 1937. He received the B.S. degree from St. Olaf College, Northfield, MN, in 1959, and the Ph.D. degree from the University of California, Berkeley, in 1965, and was a Post-Doctoral Fellow at the University of Toronto, Toronto, Ont., Canada.

He has been with Bell Laboratories, Holmdel, NJ, since 1966. His present research interests are nonlinear optics in optical waveguides and polarization preserving fibers.

John E. Bjorkholm (M'66–SM'82) was born in Milwaukee, WI, on March 22, 1939. He received the B.S.E. degree in electrical engineering-physics with highest honors from Princeton University, Princeton, NJ, in 1961, and, the M.Sc. degree in electronic sciences and the Ph.D. degree in applied physics from Stanford University, Stanford, CA, in 1962 and 1966, respectively. At Stanford, he was an NSF Graduate Cooperative Fellow and a Hughes Doctoral Fellow.

Since 1966 he has been a member of the Technical Staff at Bell Laboratories, Holmdel, NJ, where he has carried out research on various aspects of nonlinear optics and quantum electronics. Specific areas to which he has made contributions include optical parametric oscillators, distributed feedback lasers, CW self-trapping of light, two-photon spectroscopy, and resonance-radiation pressure.

Dr. Bjorkholm was Chairman of the 1977 Gordon Research Conference on Nonlinear Optics and Lasers. He is a Fellow of the American Physical Society and the Optical Society of America.

Integrated Optical Beam Splitters Formed in Glass Channel Waveguides Having Variable Weighting as Determined by Mask Dimensions

S. L. CHEN AND J. T. BOYD, SENIOR MEMBER, IEEE

Abstract—**Variable-weight beam splitters integrated into glass channel optical waveguides have been fabricated and successfully operated. Variable weighting is achieved by varying mask dimensions. Beam splitting is achieved by introducing notched reflectors of variable size into glass channel waveguides which are formed in shallow grooves having trapezoidal cross sections on silicon substrates. Preferential etching is used to fabricate these grooves and notches. A novel lift-off method incorporating a photoresist, glass, and aluminum sandwich structure is introduced to define glass channel waveguides having smooth edges within the grooves. The extent of the beam splitting notch as determined by scanning electron microscope observation is shown to correspond directly with measured beam splitting ratios for four different ratios. An insertion loss of 0.34 dB is measured for one of the samples.**

I. INTRODUCTION

BEAM SPLITTING and combining in integrated optical waveguides will likely be an important component in integrated optical devices. The capability to control the weighting of the division of an optical beam is a desirable feature. Integrated optical beam splitters allowing such control by controlling device mask dimensions are described in this paper. These beam splitters are integrated into Corning 7059 glass channel waveguides formed in shallow grooves having trapezoidal cross sections on silicon substrates. The grooves which contain the glass channel waveguides are formed by preferential etching. This etching technique is also used to form beam splitters which have a splitting ratio or weighting very close to the value expected based on simple geometric considerations.

The demonstration of variable-weight beam splitters described here along with the recent demonstrations of a temperature independent effective refractive index of the waveguide mode [1] and of very low losses achieved by laser annealing [2], [3], all using Corning 7059 glass waveguides, suggest the possibility of forming integrated optical interferometers and parallel processing filters, providing single mode channel waveguide beam splitters having as low an insertion loss as those described here could be fabricated. Such devices could combine the advantages associated with the three developments mentioned above by using 7059 glass as the waveguide material. Such devices could also use a novel lift-off method presented here for fabricating 7059 glass channel waveguides using silicon as the substrate.

Beam splitting in thin-film optical waveguides has been investigated previously by several authors. Pennington and Kuhn [4] utilized a photoresist grating fabricated on a thin-film waveguide to cause deflection of the guided beam by means of Bragg diffraction. Light deflection using the electrooptic ef-

Manuscript received November 4, 1981; revised February 18, 1982. This work was supported by the National Science Foundation under Grant ENG7617145.

S. L. Chen was with the Solid State Electronics Laboratory, Department of Electrical and Computer Engineering, University of Cincinnati, Cincinnati, OH 45221. She is now with Fairchild Semiconductor, Palo Alto, CA 94304.

J. T. Boyd is with the Solid State Electronics Laboratory, Department of Electrical and Computer Engineering, University of Cincinnati, Cincinnati, OH 45221.

0018-9197/82/0700-1072$00.75